

# BIOGEOCHEMICAL AND PHYSICAL CONTROL ON SHELF ANOXIA AND WATER COLUMN HYDROGEN SULPHIDE IN THE BENGUEL A COASTAL UPWELLING SYSTEM OFF NAMIBIA

Volker Brüchert<sup>1</sup>, Bronwen Currie<sup>2</sup>, Kathleen R. Peard<sup>3</sup>, Ulrich Lass<sup>4</sup>, Rudolf Endler<sup>4</sup>, Arne Dübecke<sup>1</sup>, Elsabé Julies<sup>1,5</sup>, Thomas Leipe<sup>4</sup> and Sybille Zitzmann<sup>1</sup>

<sup>1</sup>*Max-Planck Institute for Marine Microbiology, Celsiusstrasse 1, 28359 Bremen, Germany*

<sup>2</sup>*Ministry of Fisheries, National Marine Information and Research Centre, Strand Street, P.O. Box 912, Swakopmund, Namibia*

<sup>3</sup>*Ministry of Fisheries, Marine Research Station, 357 Lüderitz, Namibia*

<sup>4</sup>*Baltic Sea Research Institute Warnemünde, Seestrasse 15, 18119 Rostock, Germany*

<sup>5</sup>*University of Namibia, Department of Biology, Private Bag 13301, Windhoek, Namibia*

**Abstract** Shelf anoxia and recurring sulphidic water column conditions are characteristic features of the coastal upwelling system off Namibia. The development of oxygen-depleted water column conditions is linked to the relative dominance of South Atlantic Central Water, which flows southward from the Angolan Dome over Eastern South Atlantic Central Water. Inter- and intra-annual variations in the strength of upwelling influence the thickness and stability of the relatively stagnant boundary layer. Hydrogen sulphide accumulation in this boundary layer is mainly driven by the diffusive flux of hydrogen sulphide from the sediment. The hydrogen sulphide derives from the rapid degradation of organic material by bacterial sulphate reduction in the topmost 20 cm of sediment. Low reactive iron contents in the diatomaceous mud belt limit iron sulphide precipitation and sulphide oxidation by oxidized iron. In the absence of oxygen, iron, and manganese as important electron acceptors, sulphide oxidation proceeds largely by the reduction of nitrate by the large sulphur bacteria *Beggiatoa* and *Thiomargarita*, which cover large areas of the shelf. Regional differences in the distribution of these bacteria affect the development of sulphidic bottom waters. While hydrogen sulphide is quantitatively oxidized in sediments covered by *Beggiatoa* mats, only a fraction of the sulphide is removed by *Thiomargarita*. Areal estimations of aerobic water column respiration, diffusive fluxes of hydrogen sulphide from the sediment, and rates of bacterial sulphate reduction indicate that oxidation of sulphide at the sediment-water interface and oxidation of water column sulphide may comprise up to 25 % of the total oxygen consumption in the coastal

upwelling system. Advective transport of methane and hydrogen sulphide from gas-charged sediments has an intermittent and locally restricted impact on water column sulphide.

**Keywords:** Benguela, coastal upwelling, Namibia, bottom water sulphide

## 1. INTRODUCTION

Many coastal upwelling systems are characterized by year-round low-oxygen conditions in the water column and seasonal water column anoxia [17, 26, 39]. In contrast, the regular occurrence of wide spread sulphidic waters on open-ocean shelves is rare. One example is the Namibian shelf between 22°S and 27°S. Continuous upwelling between 25°30'S and 27°S in the Lüderitz cell feeds high primary production, which contributes to extreme water column oxygen depletion and episodically occurring sulphidic bottom water in the area between 25°30'S and 20°S [2, 6, 7, 11]. Turquoise discolorations of the near-shore surface waters are a regular phenomenon during the austral summer and spring. These discolorations were traditionally interpreted as coccolithophore blooms, but more recent interpretations suggest that some of these patches reflect the presence of dispersed colloidal sulphur – an oxidation product of hydrogen sulphide [40]. During the occurrence of these patches, the water column is severely oxygen-depleted and sulphidic up to the photic zone, with severe repercussions for the living resources (fish and crustaceans) in one of the largest marine ecosystems on earth [15].

A characteristic bathymetric feature of the central Benguela coastal upwelling region is a 50 to 150 km broad shelf with two edges, one at 150 m depth, and the second between 300 and 350 m water depth. Due to the high productivity and relatively shallow water depth, large amounts of phytoplankton debris reach the sea bottom before they are consumed in the water column. The large flux of organic matter permits high rates of carbon mineralization in the sediment. Since oxygen is already largely consumed in the water column, bacterial sulphate reduction becomes the dominant sediment mineralization process [7]. Ultimately, even sulphate availability is limited in these sediments, and methanogenesis starts a few centimetres below the sediment surface, which leads to the accumulation of free methane gas [14].

It is clear that the high productivity in this upwelling system is ultimately responsible for the development of free water column hydrogen sulphide. However, the pattern of hydrogen sulphide occurrence suggests very specific interactions between the dynamic oceanographic conditions, the biogeochemical processes in the sediment and water column, and the physical processes occurring within the sediment. Emeis et al. [14] suggested a close relationship between anoxia and eruptions of biogenic methane. Weeks et al. [40] also observed a sudden development of near-shore water column hydrogen sul-

phide followed by turquoise discolouration and suggested an abrupt injection of hydrogen sulphide-containing water triggered by methane eruptions from the sediment. According to Emeis et al. [14], methane gas and hydrogen sulphide in the unconsolidated sediments may be released following changes in the physical regime of the overlying water or the sediment. So far, studies have been largely descriptive and only qualitative assessments have been possible. For a quantitative analysis of the various potential sources of hydrogen sulphide – sediment or water column – regional and temporal distribution patterns of fluxes, concentrations, and budgets of hydrogen sulphide and oxygen are required. In this respect leading questions are:

1. What is the oceanic circulation pattern over the shelf and how does the chemistry of the water masses entrained in the upwelling affect overall oxygen levels on the shelf?
2. What is the rate of oxygen consumption in the water column and how does this rate compare to oxygen consumption rates at the sediment-water interface?
3. What is the regional and temporal variation in hydrogen sulphide flux in the upwelling zone and what regulates the flux from the sediments?
4. How does the gas distribution in the shelf sediment affect the flux of hydrogen sulphide from the sediment?

## 2. DATA AND METHODS

Water column and sediment data were acquired between May 1997 and May 2004 on cruises with the research vessel of the Namibian Ministry of Fisheries *RV Welwitchia* and during expeditions of the research vessels *RV Meteor*, cruises *M48-2* and *M57-3*, *RV Poseidon*, cruise *250/2*, *RV Petr Kottsov*, *Benefit* cruise and *RV Alexander von Humboldt*, cruise legs *AHAB-3* and *AHAB-4*. Station locations on the different cruises and water depths are shown on Fig. 1. A summary of the measurements is listed in Table 1. A complete table of sample locations, sampling times, and types of measurement is available from the senior author upon request. Altogether, sediment and water column data were acquired from over 130 stations.

In addition, over the course of a period of three years (May 2001 until May 2004) sediment and water column data were obtained from a shallow-water station (Station 1) at 22°50.9' S, 14°28.4' E (27 m water depth).

Continuous data records on water column physics and chemistry were obtained from a mooring that was deployed at 22°59.7'S, 14°02.8'E (131 m water depth) from December 12, 2002 until April 1, 2003 and again from January 7, 2004 until May 5, 2004.

### Bathymetry and station locations

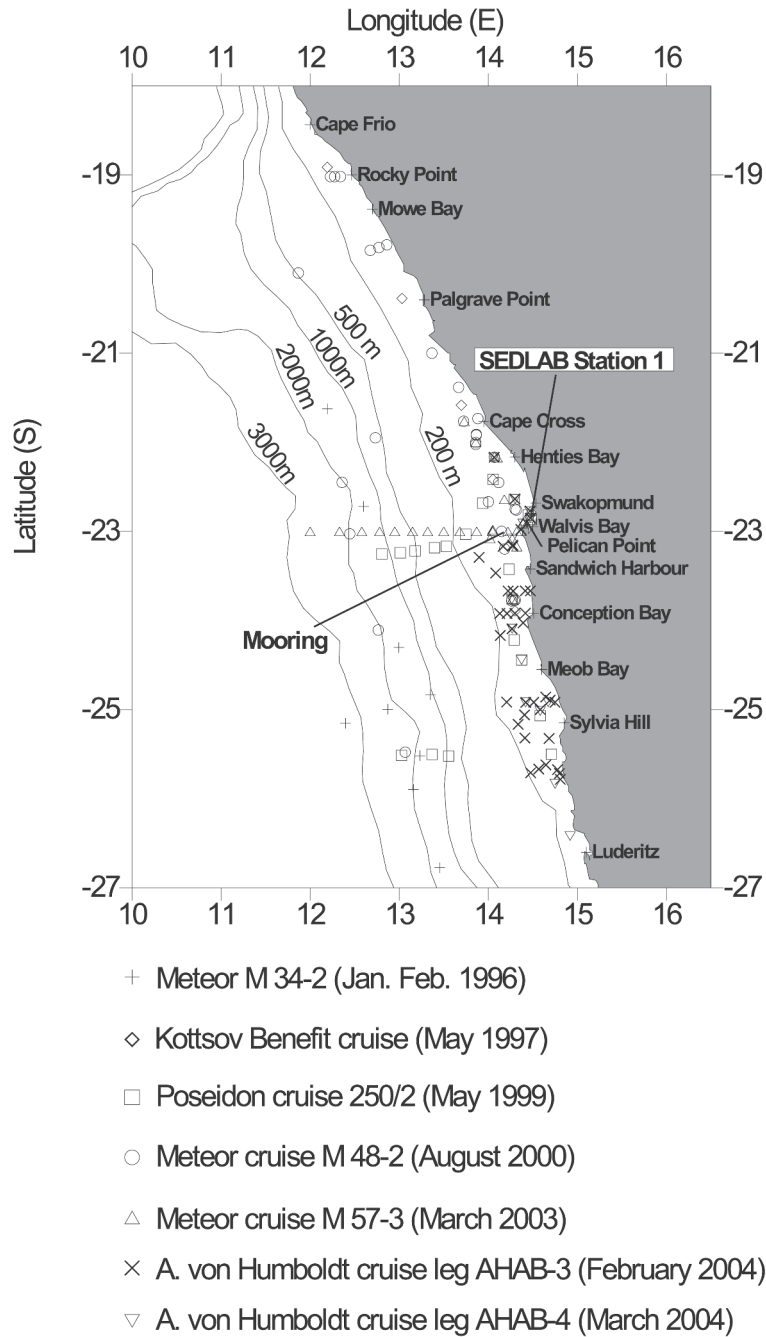


Figure 1. Bathymetry of Namibian shelf and station locations. Symbols indicate the locations of stations on the different cruises.

Table 1. Summary of biogeochemical measurements on cruises included in this survey.

	Period	Bottom water		$^{35}\text{S}$ -Sulphate reduction rates	Biomass large sulphur bacteria	
		$\text{O}_2$ ( $\mu\text{M}$ )	$\text{NO}_3^- + \text{NO}_2^-$ ( $\mu\text{M}$ )		<i>Thiomargarita</i>	<i>Beggiatoa</i>
Meteor M 34-2 cruise <sup>1</sup>	Jan-Feb 1996	+	n.d.	+	n.d.	n.d.
RV Petr Kottsov	cruise May 1997	+	n.d.	+	+	+
Poseidon 250/2 cruise	May 1999	+	+	+	+	+
Meteor M 48-2 cruise <sup>2</sup>	August 2000	+	n.d.	+	+	+
Meteor M 57-3 cruise <sup>3</sup>	March 2003	+	+	+	+	+
A. V. Humboldt cruise	Jan-March 2004	+	+	+	+	+
RV Welwitschia cruises	May 2001-May 2004	+	+	+	+	+

	Period	Oxygen		Hydrogen sulphide	
		Water column	Sediment	Water column	Sediment
Meteor M 34-2 cruise <sup>1</sup>	Jan-Feb 1996	+	+	n.d.	+
RV Petr Kottsov cruise	May 1997	+	+	+	+
Poseidon 250/2 cruise	May 1999	+	+	+	+
Meteor M 48-2 cruise <sup>2</sup>	August 2000	+	+	+	+
Meteor M 57-3 cruise <sup>3</sup>	March 2003	+	+	+	+
A. V. Humboldt cruise	Jan-March 2004	+	+	+	+
RV Welwitschia cruises	May 2001-May 2004	+	+	+	+

+ : analyzed n.d.: not determined

<sup>1</sup> Bleil et al. (1996)<sup>2</sup> Erneis et al. (2002)<sup>3</sup> Zabel et al. (2004)

## 2.1 Water Column

During the research cruises with the German vessels and RV *Welwitchia*, water column data were obtained with a CTD SBE 911+ with SBE 43 oxygen sensors, 2-channel Haardt fluorometer, a Datasonics PSA-900 altimeter with a 300 m range for bottom finding together with a rosette sampler equipped with 12 five-litre free-flow HydroBios water sample bottles. Attached to the CTD frame was an Acoustic Doppler Current Profiler (ADCP) consisting of a coupled upward- and downward-looking Workhorse ADCP 300 kHz in a 3000 dbar pressure case. Water from the HydroBios bottles was directly transferred to 120 ml Winkler bottles for duplicate determination of dissolved oxygen and sulphide. Dissolved oxygen and sulphide were determined immediately after retrieval of the rosette sampler. Dissolved oxygen was determined by Winkler titration and dissolved sulphide was determined by the method of Cline [12]. The dissolved oxygen concentrations determined by Winkler were used for calibration of the CTD SBE oxygen probe. The mooring was equipped with an upward looking 300 kHz Workhorse ADCP, four Seacat SBE 16 recorders and three Seamon temperature recorders.

## 2.2 Sediment

Sediments were collected to determine  $^{35}\text{S}$ -sulphate reduction rates, methane concentrations, fluxes of hydrogen sulphide, and abundances of the large sulphur bacteria *Beggiatoa* and *Thiomargarita*. At each station, several casts were made until sufficient material was obtained. Methods are described in detail in [7, 14]. Fluxes of hydrogen sulphide and methane were calculated from porewater profiles using the fitting procedure described by Berg et al [3]. Fluxes were calculated across the sediment-water interface. These procedures are described in detail in [7]. Distribution maps of sulphate reduction rates, sulphide fluxes, large sulphur bacteria, and bottom water oxygen and hydrogen sulphide were created with the Surfer software package using Kriging with linear interpolation as the gridding method.

Morphology, distribution, and layering of shelf sediments were investigated using the multibeam echosounder HYDROSWEEP and the PARASOUND sub-bottom profiling system on R/V Meteor. Detailed technical descriptions of the acoustic systems are given in [4, 36, 42]. A frequency of 4 kHz and a pulse length of two periods were used during the cruises. Additional measurements with different frequencies (2.5-5.5 kHz) and pulse durations of 1 to 6 periods were performed at coring stations in order to study the influence of frequency and length of the source signal on the reflection pattern. PARASOUND data were recorded continuously. High-resolution sub-bottom profiling in shallow water (up to 400 m) was performed using the parametric sediment echosounder SES96-Standard in addition to the PARASOUND device. The parametric SES96

Standard sediment echosounder is designed for operation in water depths down to 400 m. The main advantages of the SES96 echosounder are its high spatial resolution and the information contained in raw data of both HF and LF channels. This is particularly important for acoustic sediment classification in connection with the results of sediment physical property measurements.

### 3. HYDROGRAPHIC EFFECTS ON OXYGEN LEVELS IN THE COASTAL UPWELLING ZONE

The general hydrography of the Benguela Current system has been reviewed in [16, 34, 35]. More recent on-board and moored measurements have provided detailed insight into the dynamics of the regional hydrography. Two advection processes are involved in the ventilation of the subsurface water on the Namibian shelf. South Atlantic Central Water (SACW) is transported southward by the poleward undercurrent (Fig. 3a). This water originates from the area of the Angola gyre along the Namibian shelf and carries water of low oxygen ( $< 45 \mu\text{M}$ ) and high nutrient concentrations [25]. The intensity of the poleward undercurrent appears to be controlled by remote forcing in the eastern tropical Atlantic and to a lesser extent by the local wind. The second water mass is the East South Atlantic Central Water (ESACW), which is transported by the Benguela current from the area of the Agulhas retroflexion zone to the north [31]. The ESACW is well-ventilated and has a lower nutrient concentration than the SACW. Sub-thermocline cross-shelf circulation advects ESACW in depths between 20 and 70 m from the area off the shelf break onto the shelf (Fig. 3b). This transport is mainly driven by the local alongshore wind stress and compensates for the Ekman offshore transport in the surface layer (Fig. 3b). Since the oxygen concentration of the ESACW water is higher, advection by cross-shelf circulation ventilates the intermediate waters on the shelf much more efficiently than the advection by the poleward undercurrent. The oxygen concentration of the subsurface water on the shelf is very sensitive to the local balance of consumption and ventilation processes, which both shape the pattern of oxygen concentration and its variation in space and time.

Upwelling-favourable winds on the Namibian shelf are strong in the Cape Frio and Lüderitz upwelling cells and weak in the area between the upwelling cells. While the northern part of the Benguela is strongly affected by the advection of SACW with the poleward undercurrent, with increasing distance from the Angola-Benguela front, the cross-shelf circulation in the subsurface shelf water gradually increases the proportion of ESACW. Cross shelf circulation intensifies in the Lüderitz upwelling cell such that well-ventilated ESACW becomes the dominating water mass on the shelf and limits the southward extension of SACW to the latitude of Lüderitz, where the subsurface shelf waters consist entirely of ESACW. Upwelled water of the Lüderitz cell is also ad-

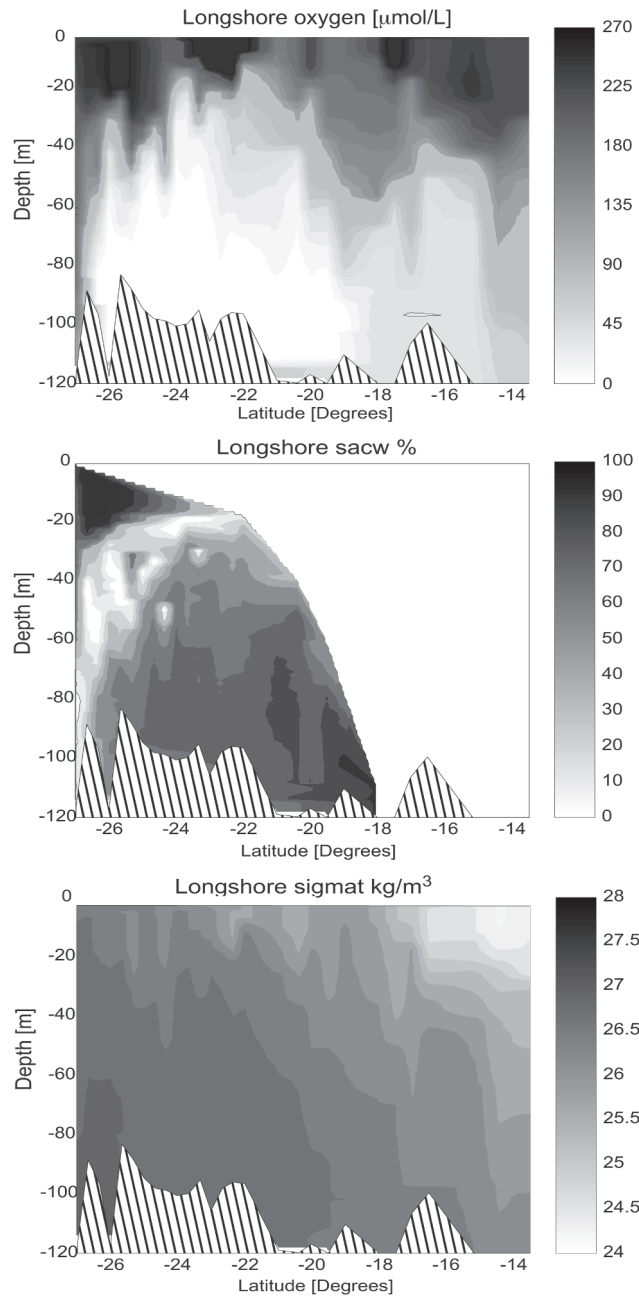


*Figure 2.* Density, oxygen, and percentage of SACW in a alongshore transect from 13°S to 27°S based on volumetric temperature-salinity (T-S) analysis. Water masses outside the definition of the ESACW-SACW T-S field are not shown.



vected northward by the surface current and causes a northward displacement of the most productive area by a few degrees latitude. This displacement is associated with a northward shift of the area of the most extreme subsurface oxygen depletion produced by the respiration of sinking organic matter to the area around 24°S (Fig. 2).

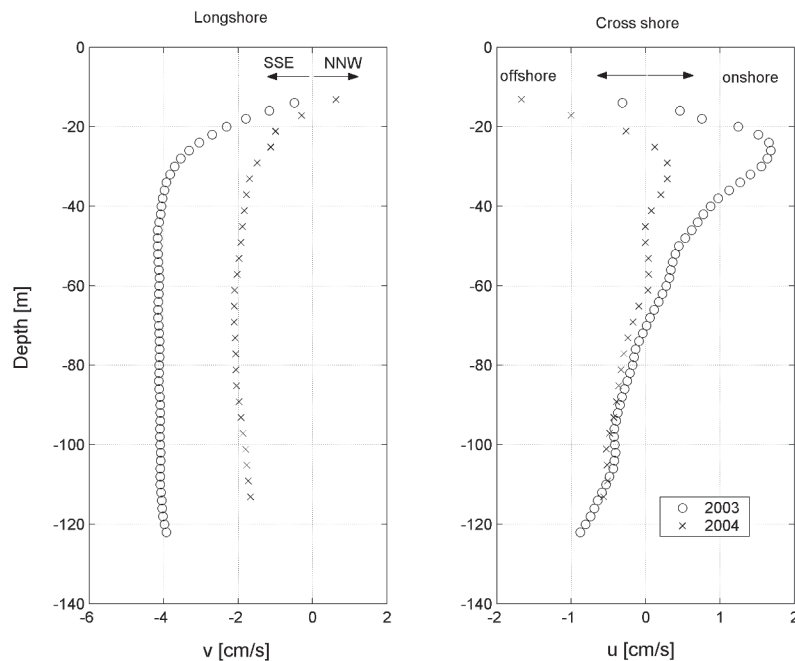


Figure 3. Averaged alongshore (a) and cross-shore (b) current velocity at the mooring (22° 59.7' S, 14° 02.8' E, 131 m water depth) located in the mud belt off Walvis Bay. The mooring was deployed from December 9, 2002 until April 1, 2003, and from January 7, 2004 until May 5, 2004.

Data from the mooring in 130 m water depth at 23°S indicate interannual variations in the strength of the poleward undercurrent located below 20 m water depth (Fig. 3a, b). In the period December 2002 until April 2003, the meridional (southward) component had average current speeds of  $4 \text{ cm s}^{-1}$ , but for the period January 2004 until May 2004, the current speed was averaging only  $2 \text{ cm s}^{-1}$  (Fig. 3a). Similarly, the cross-shelf circulation represented by the zonal component of the current varied between the two observation periods (Fig. 3b). On-shore transport was weaker in 2004 compared to 2003 indicating that the ventilation by ESACW in the intermediate layer was weaker in the austral fall of 2004.

The mooring data indicate a transient, sluggish bottom water layer of up to 30 m thickness. This layer appears to be stable for months. The slower the meridional current component, the longer the residence time on the shelf, the more this layer becomes oxygen- and nitrate-depleted, and ultimately sulphidic. At coast-parallel bottom current speeds of 2 and 4 cm s<sup>-1</sup>, water is transported within approximately 600 and 300 days, respectively, from the Angola-Benguela front to 26°S. Hence, this period can be taken as an approximate residence time for shelf bottom water reaching 26°S.

## 4. PATHWAYS, RATES, AND AMOUNT OF WATER COLUMN RESPIRATION

### 4.1 Aerobic Water Column Respiration

Generally, oxygen concentrations decrease rapidly below the thermocline on the shelf as a result of the aerobic respiration of sinking organic material. Video observations from a remotely operated vehicle during RV METEOR Expedition M57-3 in March 2003 suggest that particulate organic material in the water column over the shelf consists mostly of aggregates [42]. We have used a new approach to estimate the rate of oxygen consumption in the water column by combining volume-specific oxygen consumption rates of diatom aggregates with abundances and size spectra of aggregates determined by in-situ video observation during a diatom bloom in the southern Benguela system [20]. Size-dependent rates of diffusive oxygen uptake in diatom aggregates have been determined by [30]. Diffusive oxygen uptake varied as a function of aggregate size, and was described by the relationship  $Q_{tot,vol} = 65.8(vol)^{0.67}$ , where  $Q_{tot,vol}$  is the total oxygen consumption (nmol agg<sup>-1</sup> h<sup>-1</sup>) as a function of aggregate volume (vol) [30]. The above equation can be recast as a function of aggregate radius, which yields the expression

$$Q_{tot,r} = 171r^{2.0} \quad (1)$$

where  $Q_{tot,r}$  has the unit nmol O<sub>2</sub> cm<sup>-3</sup> h<sup>-1</sup>. Extrapolation of the aggregate radius-specific respiration rate to a respiration rate per volume seawater requires that the aggregate size spectrum in the water column is known. We used the empirical relationship reported in Kiørboe and co-workers [20] for a diatom bloom in the southern Benguela. The aggregate size spectrum was described by the power function

$$n_r = b_3 r^{-b_4} \quad (2)$$

where  $n_r$  represents the volume-normalized number of aggregates, the subscript  $r$  is the aggregate radius,  $b_3$  is a particle concentration coefficient and  $b_4$  describes the slope of the spectrum [19]. The larger  $b_4$ , the smaller are the

particles. The total respiration by aggregates (Total  $R_{agg}$  across a complete size spectrum was determined by integrating equations (1) and (2) to yield the expression

$$Total R_{agg} = \int_{r_1}^{r_2} n_r Q_{tot,r} dr = \frac{b_3 * 171}{2.0 - b_4 + 1} r^{2.0-b_4+1} \quad (3)$$

We used published values of  $b_3$  and  $b_4$  for the diatom bloom reported in Kiørboe and Jackson [19]. These values are  $1 \times 10^{-4}$  and  $1.3 \times 10^{-3}$  for  $b_3$ , and 1.6 and 2.6 for  $b_4$ , respectively. Mean values for  $b_3$  and  $b_4$  are  $7.5 \times 10^{-4}$  and 2.1, respectively. The reported aggregate size spectrum ranged from 0.225 mm to 5 mm [20]. The calculated respiration rates vary between 0.1 and  $7.7 \mu\text{M O}_2 \text{ day}^{-1}$  with a mean of  $1.7 \mu\text{M day}^{-1}$ . These average oxygen consumption rates translate into depth-integrated oxygen consumption rates of 52, 96, 172  $\text{mmol O}_2 \text{ m}^{-2} \text{ day}^{-1}$  for water depths of 30, 50, and 100 m depth, respectively. Decreasing particle abundances with depth and variations in the intensity and the temporal and spatial extent of blooms in the Benguela current [10, 16] introduce uncertainties to our method that are difficult to quantify at the moment. Yet, this method for the calculation of oxygen consumption is superior over other approaches such as the apparent oxygen utilization in that it is independent of variations in the oxygen concentration of the source waters feeding the upwelling system.

## 4.2 Anaerobic Water Column Processes

Nitrate is a potential electron acceptor for the respiration of organic matter in the absence of oxygen and may serve as electron acceptor for the oxidation of dissolved sulphide, when oxygen is depleted. Thus, the development of sulphidic bottom waters may require the complete consumption not only of oxygen, but also of dissolved nitrate. Long-term records of bottom water nitrate and hydrogen sulphide indicated highly variable nitrate concentrations in the bottom water of the Namibian shelf. Hydrogen sulphide was detected in the coastal inshore bottom waters (25m depth) in May 2001 and 2004, and during these periods, nitrate was absent from the shelf bottom waters (Fig. 4). However, there were also periods when sulphide was absent and nitrate was very low, e.g., January 2003, and when sulphide and nitrate co-existed, albeit at very low concentrations, e.g. September 2003 (Fig. 4). One possible explanation is that the bottom water was in a transitional stage during these sampling times.

An extensive data set of the Sea Fisheries Institute of South Africa and the Ministry of Fisheries, Namibia indicates a permanent deficit of nitrate relative to phosphate and silicate in the coastal upwelling waters. The nitrate deficit

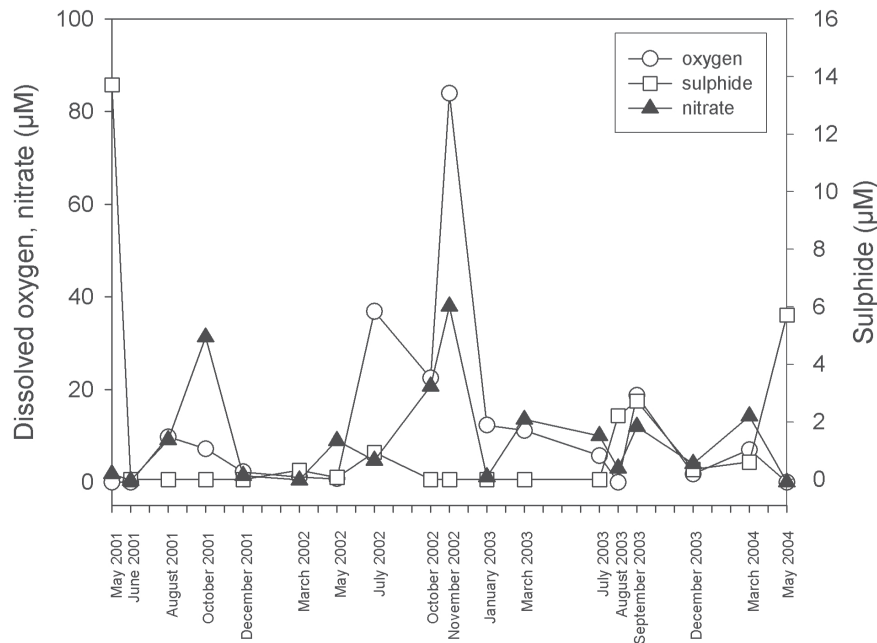


Figure 4. Time series of bottom water oxygen, nitrate, and hydrogen sulphide at SEDLAB Station 1 from May 2001 until May 2004.

defined as  $\Delta N = 16[\text{PO}_4^{3-}] - [\text{NO}_3^-]$  is most extreme in the in-shore areas in the Northern Benguela near 23°S [38]. Tyrell and Lucas [38] interpreted this deficit as the anaerobic respiration of organic matter with nitrate as electron acceptor, i.e., denitrification. However, direct tracer measurements using  $^{15}\text{N}$ -labelled nitrate and ammonium do not support this interpretation. Anammox, a recently discovered anaerobic bacterial process in anoxic water columns, which catalyzes the consumption of nitrate/nitrite together with ammonium to form  $\text{N}_2$ , appears to be the main process for nitrogen removal in the oxygen deficient water column of the Namibian shelf [21]. Irrespective of which bacterial process is ultimately responsible for nitrogen removal, our current data suggest that complete bottom water nitrate depletion is a common corollary of sulphidic bottom waters.

The only direct measurements of bacterial sulphate reduction with radiolabelled  $^{35}\text{S}\text{-SO}_4^{2-}$  in bottom waters (3 m above ground) were performed at four shelf stations in March 2004. During this period, bottom waters were anoxic, but did not contain hydrogen sulphide. The experimental rates ranged from 0.2 to 6.8  $\text{nmol l}^{-1} \text{day}^{-1}$ . At the highest rates, it would require 147 days to

reach a concentration of  $1\mu\text{M}$  hydrogen sulphide, the detection limit for the methylene blue method [12]. Measured hydrogen sulphide concentrations in the water column have been as high as  $40\mu\text{M}$ , but have been observed to rise and disappear much faster than 147 days (see section 5.3).

## 5. BACTERIAL SULPHATE REDUCTION, METHANOGENESIS, FLUXES, AND RECYCLING OF SULPHIDE AT THE SEABED

### 5.1 Carbon Oxidation Processes and Methanogenesis

Sediments on the Namibian shelf generally contain less than 20 percent clastic material, which is transported mainly as dust from the Namibian desert. Minerals containing reactive iron and manganese oxide are minor components of the sediment, with the consequence that these two anaerobic electron acceptors are quantitatively unimportant for carbon oxidation [5]. Rates of nitrogen removal including denitrification in the shelf sediments range from 0.2 to 2.7  $\text{mmol m}^2 \text{ day}^{-1}$ , averaging  $2 \text{ mmol m}^{-2} \text{ day}^{-1}$  (Zitzmann and Brüchert, unpubl. data). This leaves bacterial sulphate reduction as the dominant terminal organic carbon oxidation process. Areal rates of bacterial sulphate reduction on the shelf (28 m to 200 m water depth) vary between 3.1 and  $62.7 \text{ mmol m}^{-2} \text{ day}^{-1}$  [7].

On average, more than 90 % of bacterial sulphate reduction takes place in the top 10 cm of sediment indicating a very reactive pool of organic material (Fig. 5). However, the amount of remaining organic material below 10 cm sediment depth is still very large. Sulphate reduction continues below 10 cm depth at low rates until all sulphate is consumed and methanogenesis starts. Rapid increases in methane concentration lead to methane saturation only centimetres below the sediment-water interface (Fig. 6). Steep opposing gradients of porewater methane and sulphate indicate anaerobic oxidation of methane coupled to sulphate reduction [14]. In the absence of reactive iron oxides, the capacity for precipitation of dissolved sulphide as iron sulphides is limited, and slowly forming organic sulphides remain as the only significant sediment sink for hydrogen sulphide [5, 8]. These conditions explain, why concentrations of dissolved sulphide in porewaters from Namibian shelf sediments can be as high as 22 mM at only 10 cm sediment depth (Fig. 6), and consistently exceed 2 mM at 6 cm depth in all currently analyzed sediments between  $19^\circ\text{S}$  and  $27^\circ\text{S}$  on the shelf.

### 5.2 Sulphide Oxidation

In most marine sediments, a significant amount of hydrogen sulphide can be oxidized with iron and manganese oxides [1, 32, 37]. Low concentrations of reactive iron and manganese in the Namibian shelf sediments limit the

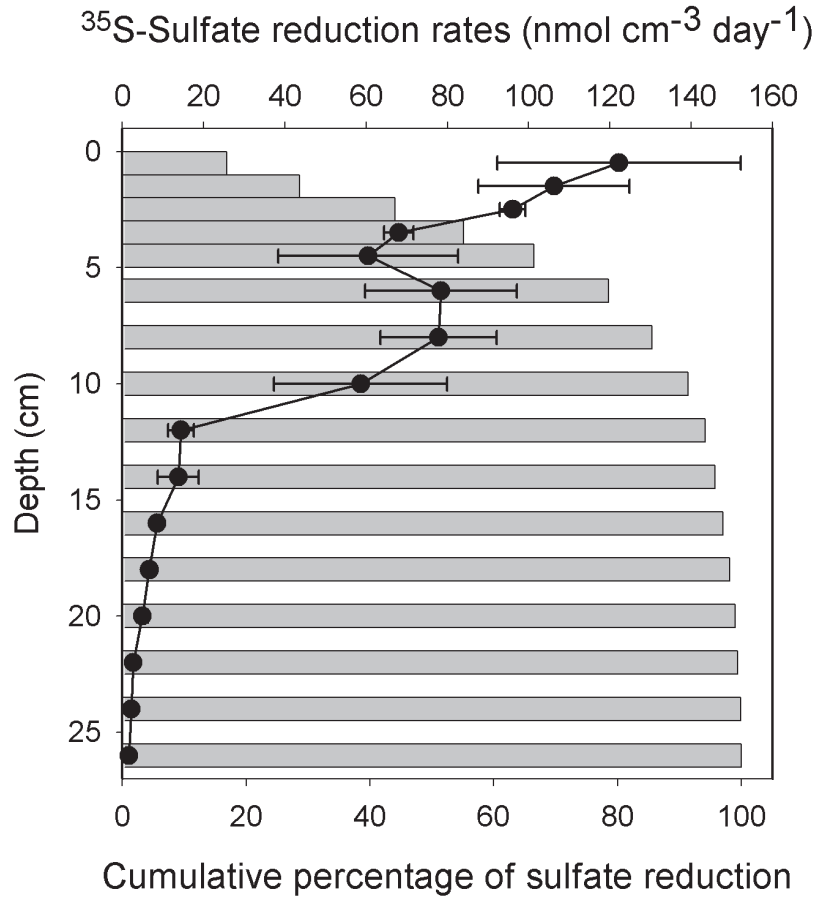


Figure 5. Representative depth profile of <sup>35</sup>S-sulphate reduction rates and cumulative percentage of sulphate reduction, here shown for M57-3 Station 178, March 2003.

oxidation of hydrogen sulphide to dissolved oxygen and nitrate. Since oxygen concentrations are already very low near the sediment-water interface, the major amount of hydrogen sulphide oxidation must take place by the reduction with nitrate. Studies of the large sulphur bacteria *Thioploca*, *Beggiatoa*, and *Thiomargarita* over the past 10 years have indicated their capacity for using nitrate as an alternative electron acceptor [24, 29]. Adaptations such as the intracellular storage of nitrate and elemental sulphur in vacuoles enable the bacteria to survive periods when electron donor and acceptor are limited in the ambient environment. The intracellular storage of nitrate may allow the bacteria to survive for up to 8 months [33]. Although the actual survival period of the bacteria in nature is uncertain, the principal conclusion is that sulphide oxidation can be decoupled from the contemporaneous presence of nitrate or

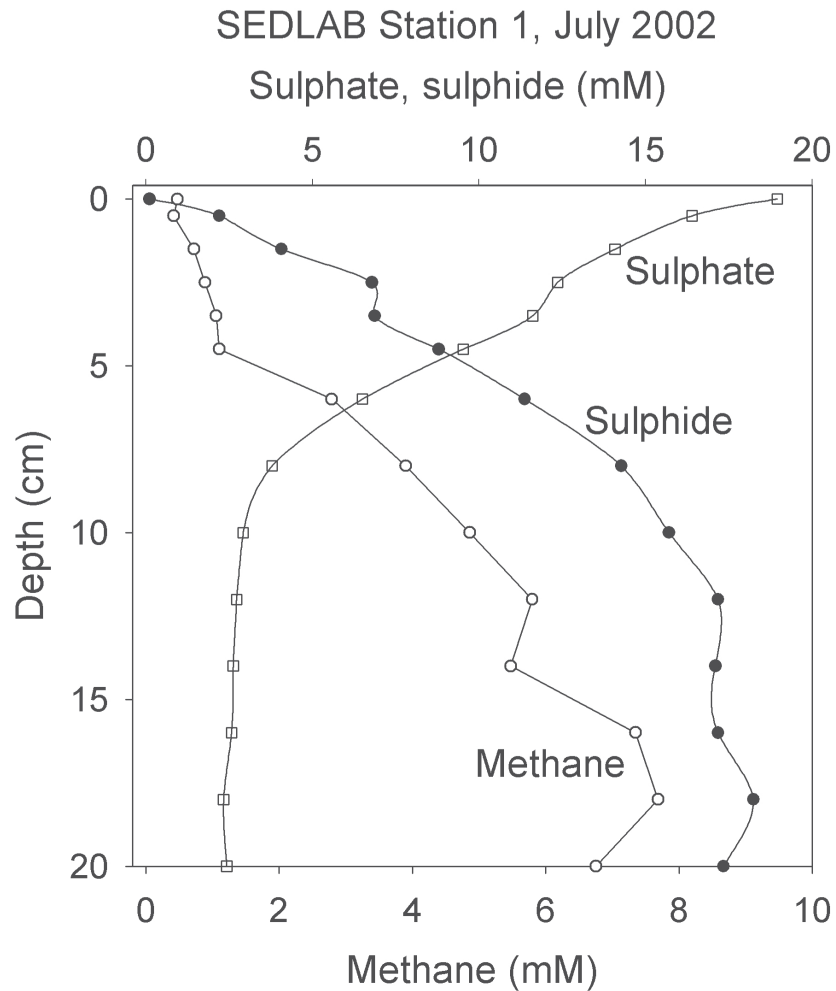


Figure 6. Representative depth profile of dissolved sulphate, sulphide, and methane concentration, here shown from SEDLAB Station 1, July 2002. Methane (○), sulphide (●), sulphate (□).

oxygen in the bottom waters. Therefore, sulphide oxidation can take place even when there is no dissolved nitrate or oxygen measurable in bottom waters because the large sulphur bacteria can retain a pool of intracellular nitrate to bridge periods with low or absent bottom water nitrate.

Experimental data indicate that a biofilm of *Beggiatoa* can quantitatively oxidize hydrogen sulphide [27], which is also in accordance with field microsensor measurements through *Beggiatoa* mats from Namibian shelf sedi-

ments that indicate complete removal of hydrogen sulphide in the mats (Stief and Brüchert, unpubl. data). Brüchert et al. [7] used data from 12 shelf stations to calculate the percentage of the hydrogen sulphide flux relative to bacterial sulphate reduction and found that between 4 and 51% of formed hydrogen sulphide diffuses across the sediment-water interface. In the presence of *Beggiatoa*, no hydrogen sulphide enters the water column, while *Thiomargarita* may reduce the diffusive upward sulphide flux by up to 45% [7]. The different physiological adaptations of these two bacterial species to hydrogen sulphide fluxes and concentrations make them good indicators for differences in the severity of bottom water anoxia and the potential occurrence of bottom water sulphide.

### 5.3 Regional Distribution

Fig. 7a shows the areal distribution of bacterial sulphate reduction rates on the Namibian shelf and slope. Areas with enhanced bacterial sulphate reduction correspond to areas of retention rather than to upwelling cells such as the Lüderitz upwelling cell. In the Lüderitz cell upwelling is almost perennial [9, 10]. Since upwelling mixes the water column in the cell continuously, phytoplankton biomass is not as high as further north, where the water column can become weakly stratified and water retention is higher [2]. As a consequence, rates of organic matter accumulation are also smaller in the Lüderitz cell. As less phytoplankton reaches the seafloor, and bottom water ventilation is better due to the upwelling of ESACW, rates of bacterial sulphate reduction in the sediment are correspondingly lower.

Diffusive hydrogen sulphide fluxes are always a fraction of the bacterial sulphate reduction rates (Fig. 7b). The highest fluxes are restricted to three areas: (1) Between 25°S and 24°S extending approximately from Sylvia Hill to Meob Bay, (2) from 23°30'S to 22°50'S, i.e., Conception Bay to Pelican Point including the area of Walvis Bay, and (3) the area from Cape Cross to Henties Bay. There is no significant agreement between the rates of bacterial sulphate reduction and hydrogen sulphide fluxes. South of Walvis Bay, the rates of sulphate reduction and the hydrogen sulphide fluxes roughly correlate, whereas to the north, none of the areas with enhanced bacterial sulphate reduction are evident in the hydrogen sulphide flux pattern. The highest hydrogen sulphide fluxes only coincide in the area inside Walvis Bay and are generally restricted to a very small area.

The distribution pattern of the large sulphur bacteria can provide answers to these discrepancies. *Beggiatoa* and *Thiomargarita* are concentrated in different areas, respectively (Fig. 8a and 8b). *Beggiatoa* is concentrated in the area north of Palgrave Point and is found north to Cape Frio, whereas *Thiomargarita* is most abundant in the area south of Palgrave Point and around Walvis Bay.



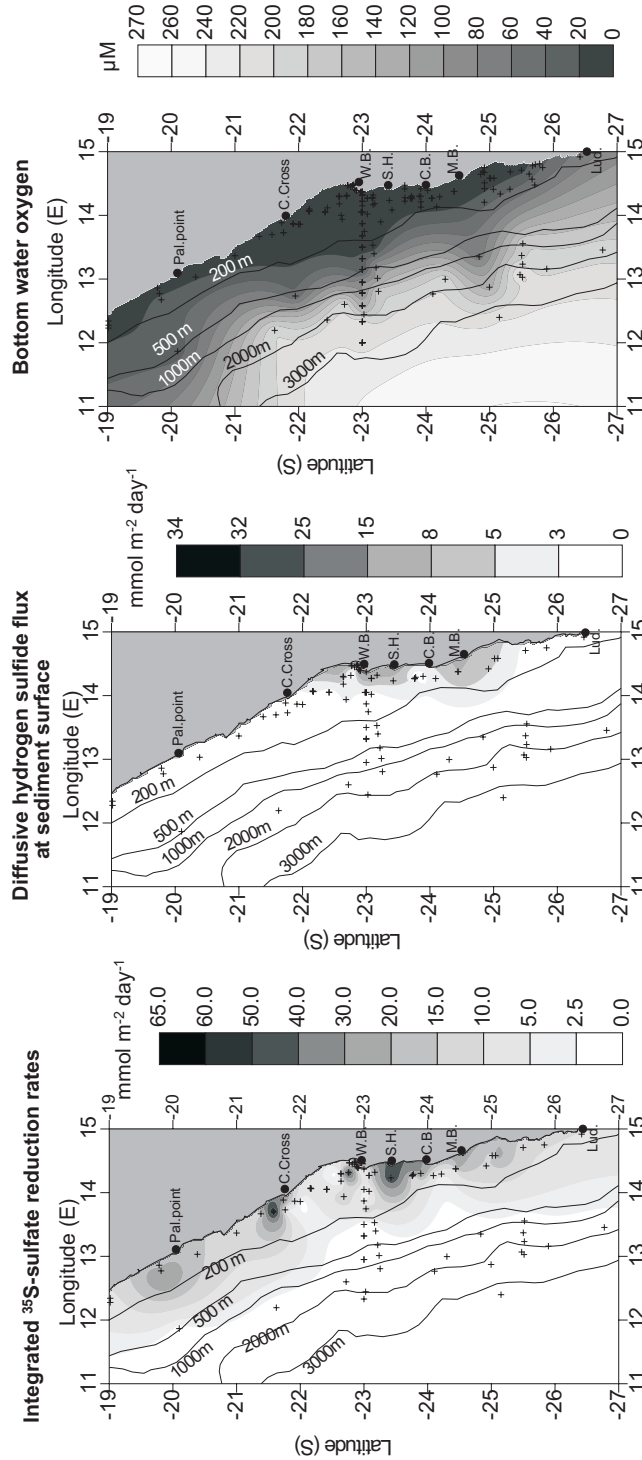


Figure 7. Areal distribution map of (a) depth-integrated bacterial sulphate reduction rates, (b) diffusive hydrogen sulphide fluxes across the sediment-water interface, (c) annually averaged bottom water dissolved oxygen concentrations.

*Thiomargarita* and *Beggiatoa* are also abundant south of Walvis Bay between 24°S and 25°30'S near Sylvia Hill and between Conception Bay and Walvis Bay. The distribution maps represent quasi-averages over 7 years of observation. It is important to note that significant intra- and interannual fluctuations in abundance exist. These are integrated into the maps for the areas where stations were revisited several times.

Field observations have consistently shown that *Beggiatoa* is absent from areas with bottom water hydrogen sulphide. *Thiomargarita*, in contrast, can tolerate hydrogen sulphide at least temporarily at millimolar concentrations and has been found to survive in environments repeatedly containing bottom water hydrogen sulphide [7]. This is confirmed by the distribution map of *Thiomargarita* and the areas where bottom water hydrogen sulphide has been found on the Namibian shelf (Fig. 8c). The difference in distribution between the two types of large sulphur bacteria may have to do with the slower metabolism of *Thiomargarita* relative to *Beggiatoa*, when growing with nitrate. The large size of *Thiomargarita* may allow them to store larger amounts of nitrate and survive for longer time periods under adverse conditions.

#### 5.4 Temporal Variation

We assessed the intra- and interannual variability at a selected station in shallow depth (28 m), with shallow gas saturation (SEDLAB Station 1). Between May 2001 and May 2004, concentrations of porewater methane, hydrogen sulphide, and water column oxygen were determined nearly every two months (Fig. 9a-c). At this sampling frequency marked fluctuations in oxygen levels in the water column were detected, in concert with variations in methane concentration and with fluxes of hydrogen sulphide. There was no apparent periodicity in the observed fluctuations, and except for one period oxygen concentrations in the bottom water were below 22  $\mu\text{M}$ . The most conspicuous feature was the extreme oxygen depletion over the whole water column, with drops in surface concentrations of oxygen to values as low as 67  $\mu\text{M}$ . A relatively stable chemocline was only present during the austral summer 2001/2002 (October 2001 until May 2002). During this period, two low-oxygen periods occurred in December 2001 and in May 2002. Oxygen-rich water intruded after May 2002, but was interrupted by another low-oxygen period in October 2002, which was also terminated abruptly. Subsequently, oxygen levels dropped in the bottom water and the chemocline rose gradually throughout the year 2003 reaching the shallowest depth in March 2004. Data acquisition stopped in May 2004 with an apparent return to better ventilated conditions.

During time periods when a shallow chemocline was present, methane concentrations increased abruptly in the sediment so that the depth of methane

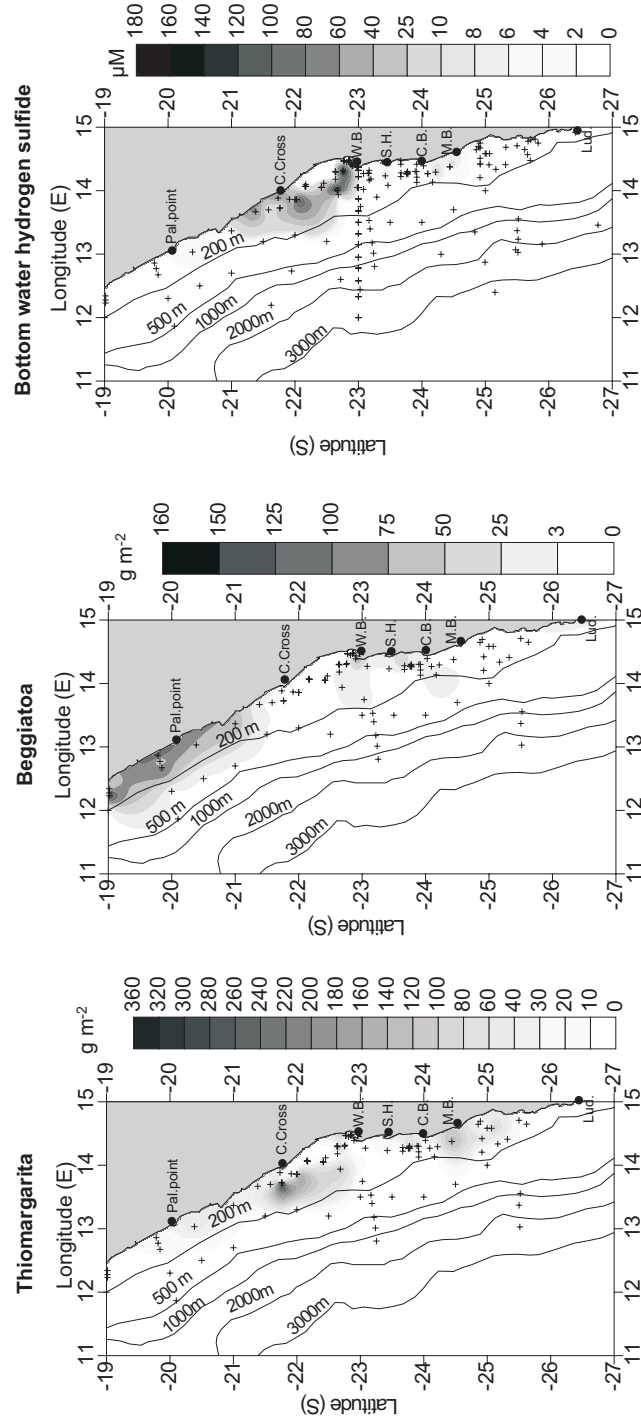


Figure 8. Areal distribution map of (a) Thiomargarita, (b) Beggiatoa, (c) annually averaged bottom water hydrogen sulphide.

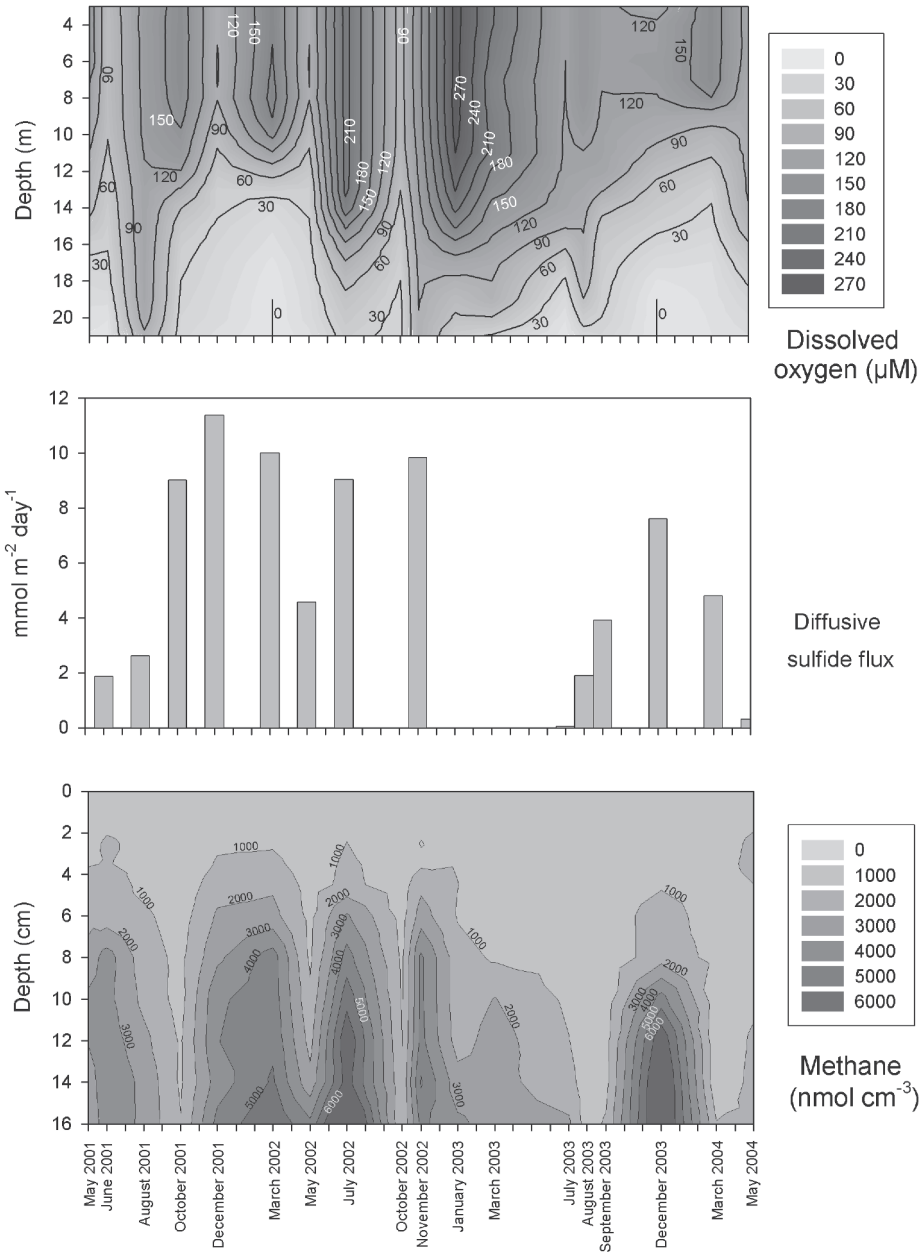


Figure 9. Time series plot from SEDLAB Station 1 of (a) water column dissolved oxygen, (b) diffusive sulphide flux, (c) sediment methane concentrations.

saturation rose to a sediment depth as shallow as 4 cm. Sulphide fluxes also increased during these periods. The sulphide fluxes ranged from 0.02 to 11.4 mmol m<sup>-2</sup> day<sup>-1</sup>, a variation of more than 2 orders of magnitude. The enhanced sulphide fluxes and methane concentrations did not coincide with the punctuated low-oxygen periods. In two cases, the low-oxygen period preceded the period of increased methane and sulphide fluxes. It appears that the period of good stratification was conducive for the accumulation of bottom water hydrogen sulphide (Fig. 4). Nitrate concentrations, which were below the detection limit in March 2002, support this interpretation. There was no bottom water hydrogen sulphide before March 2002, but it may have been missed because of the relatively long sampling gap. Coincidentally, during the summer 2001/2002, there were numerous observations of turquoise near-shore surface water discolorations and hydrogen sulphide smell suggesting that hydrogen sulphide was present in the water column [40]. It is clear that a higher sampling frequency than once every two months is required in order to capture the true dynamic nature of developing anoxia.

### 5.5 The Contribution of the Sedimentary Microbial Sulphur Cycle to System-Wide Oxygen Consumption

Overall oxygen consumption in the Namibian upwelling system takes place by aerobic respiration of organic material in the water column, hydrogen sulphide oxidation at the sediment-water interface, and oxidation of water column hydrogen sulphide. The proportions of these processes vary as a function of water depth, spatial occurrence of water column hydrogen sulphide and sulphide-oxidizing bacteria, and sediment sulphate reduction rates. We have divided the shelf into the total shelf and the inner shelf area, which we defined as the areas inside the isobaths of 300 m and 100 m, respectively. Table 2a shows that extreme anoxia (oxygen concentrations less than 1  $\mu$ M) only occur in an area covering 8944 km<sup>2</sup>, roughly 10 % of the total shelf area. Bottom waters characteristic of hypoxic conditions (< 22.3  $\mu$ M/0.5 ml/l) cover 46954 km<sup>2</sup>, which is 55 % of the total shelf and an area larger than the inner shelf (21690 km<sup>2</sup>). With few exceptions, hydrogen sulphide diffuses across the sediment-water interface only in areas of the inner shelf. For an estimate of the relative proportions of oxygen-producing and oxygen-consuming processes, area-integrated fluxes were calculated for oxygen production and consumption for the inner and total shelf, respectively (Table 2b). Oxygen production by photosynthesis and the import of oxygen by upwelling amount to 10.9 x 10<sup>9</sup> and 24.8 x 10<sup>9</sup> moles O<sub>2</sub> day<sup>-1</sup> for the inner and total shelf, respectively (Table 2b). Aerobic water column respiration (1.8 and 21.7 x 10<sup>9</sup> moles O<sub>2</sub> day<sup>-1</sup>) balances 16.5 % and 87.5 % of the photosynthetic oxygen production/import in the two areas, respectively. The combined water column and benthic sulphide

oxidation contributes 25 % and 9 % to the total oxygen consumption on the inner and total shelf, respectively. This comparison emphasizes the importance of sedimentary processes for the regulation of water column oxygen levels on the inner shelf. Although there are considerable uncertainties associated with the estimation of water column respiration, there is a reasonable match between the combined sediment and water column oxygen consumption versus primary production and import of oxygen, which gives further support to our estimates.

*Table 2.* Areal and volumetric estimates of Namibian shelf area between 29°S and 17°S, inventory of oxygen and water column hydrogen sulphide, and areal occurrence of sulphur bacteria.

<i>Areal estimates</i>	<i>Area (km<sup>2</sup>)</i>
Shelf area (max. 300 m water depth) 29°S to 17°S	85472
Shelf (max. 100 m water depth) 29°S to 17°S	21690
Gas-charged area	1350
Area covered by craters, domes, and disrupted sea floor	380
Hydrogen sulphide, bottom water, > 1μM, 10 - 30 m thickness	27978
Bottom water dissolved oxygen, <44.6μM (1 ml/l)	78565
Bottom water dissolved oxygen, <22.3μM (0.5 ml/l)	46954
Bottom water dissolved oxygen, <11μM (0.25 ml/l)	31491
Bottom water dissolved oxygen, <1μM (0.022 ml/l)	8944
Thiomargarita >5 gm <sup>-2</sup> biomass	50555
Beggiatoa, >5 g m <sup>-2</sup> biomass	33143

## 6. SEDIMENTOLOGICAL CONTROL ON SULPHATE REDUCTION RATES AND METHANE ACCUMULATION

Three main regions with different sediment patterns were outlined from the acoustic records. The continental slope consists of soft silts forming a smooth surface with westward prograding sediment layers. At the shelf break the sea bottom consists of hardground and consolidated sediments suggesting a non-depositional environment. Well-stratified deposits with dipping reflectors are truncated and partly covered with silty/sandy sediments (Fig. 10). Strong bottom currents prevent the deposition of soft sediments. These sediments are apparently reworked deposits. They contain only small amounts of reactive organic material and support relatively low depth-integrated rates of sulphate reduction that are less than 1.5 mmol m<sup>-2</sup> day<sup>-1</sup> [7]. Porewater concentrations of dissolved sulphide are in the low μM range, and fluxes of hydrogen sulphide across the sediment-water interface are below detection. In addition, at depths greater than 150 m, no large sulphur bacteria have been observed [7].

Table 3. Area-integrated flux estimates of oxygen production and consumption due to respiration and sulphide oxidation for the Namibian shelf between 29° S and 17° S.

Source/sink	Inner shelf ( < 100 m water depth)	Total shelf ( < 300 m water depth)
	O <sub>2</sub> production (+) / consumption (-) 10 <sup>9</sup> moles day <sup>-1</sup>	
Estimated integrated primary production <sup>(1)</sup>	4.7	18.6
Import of oxygen with upwelling waters and poleward undercurrent <sup>(2)</sup>	6.2	6.2
Aerobic respiration in the water column <sup>(3)</sup>	-1.8	-21.7
Oxygen consumption of sulphide diffusing into the water column <sup>(4)</sup>	-0.1	-0.3
Sediment oxygen uptake for benthic sulphide oxidation <sup>(4,5)</sup>	-0.5	-1.9

<sup>1</sup> Primary production: 217 mmol C m<sup>-2</sup> day<sup>-1</sup> based on 0.37 Gt C yr<sup>-1</sup> (Carr, 2002) for an area covering 389,000 km<sup>2</sup>; Org. C : O<sub>2</sub> production (1:1)

<sup>2</sup> Upwelling: 1.6 Sv [34], O<sub>2</sub> concentration: 45 μM

<sup>3</sup> Based on experimental oxygen consumption rates of 1.7 μM day<sup>-1</sup> (see text)

<sup>4</sup> expressed in O<sub>2</sub> equivalents (mole O<sub>2</sub> : mole H<sub>2</sub>S = 2:1)

<sup>5</sup> Calculated as the difference between depth-integrated sulphate reduction rate, diffusive hydrogen sulphide flux, and sulphide burial (see [7])

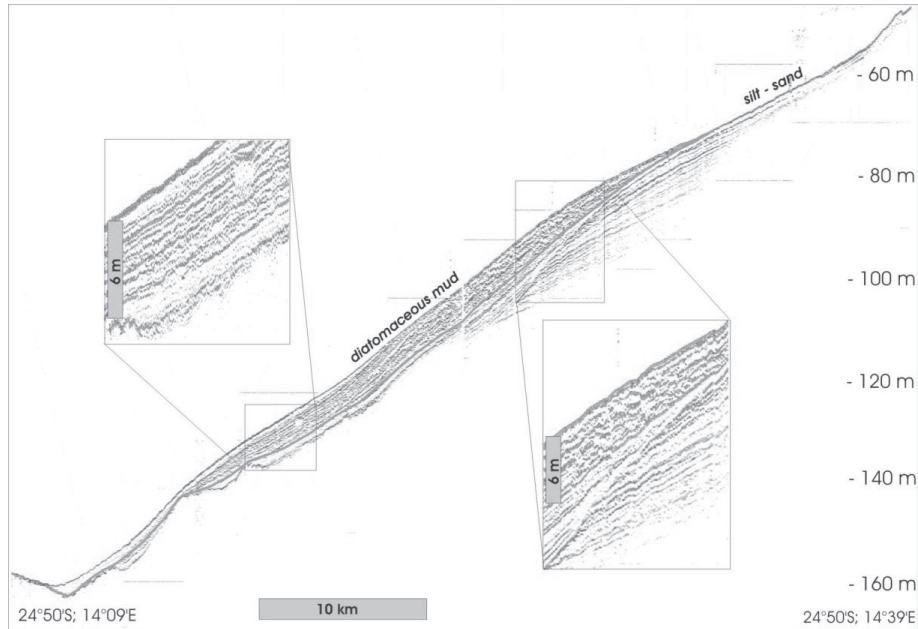


Figure 10. SES96 Sediment echosounder profile 1: cross section of the mud belt at 24°50S showing stratified, gas-free mud over westward prograding sandy layers. Towards the coast, at a depth of about 70 m, the muddy surface sediment changes to coarser (silt, sand) material.

The near-shore region (water depths of less than 150 m) is characterized by sedimentation of organic matter forming a NNW-SSE striking (coast parallel) diatom mud layer, which grows to more than 10 m thickness towards the coast (Fig. 11). At water depths between 80 m and 130 m, acoustic anomalies, so-called blankings, occur that indicate free gas accumulations at about 6 m depth in the mud layer (Fig. 11). The gas bubbles are concentrated under a less permeable layer inside the mud. Comprehensive acoustic investigations on gas-charged mud in Eckernförde Bay, Baltic Sea, used similar acoustic frequencies to our study [41] and found that between 2% (mean) and 8% of the pore space are occupied by bubbles.

In direction to the coast, the isolated acoustic gas blankings change into a permanent gas-charged layer at about 3 to <1 m sub-bottom depth. This gas-charged layer intersects the sea-bottom at water depths of about 40 m (Fig. 11). Near the coast, between 22° 50'S and 23° 10'S, east of 14° 15'E the flat sea bottom changes to morphological features like pockmarks (Fig. 11) and very rough sea bottom surface (Fig. 11). These features indicate recent eruptions of free gas and/or gas-charged mud blocks. Upward-travelling gas bubbles in the water column from one of the pockmarks were observed in the high-frequency channel of the SES96 echosounder during station work. The area affected by



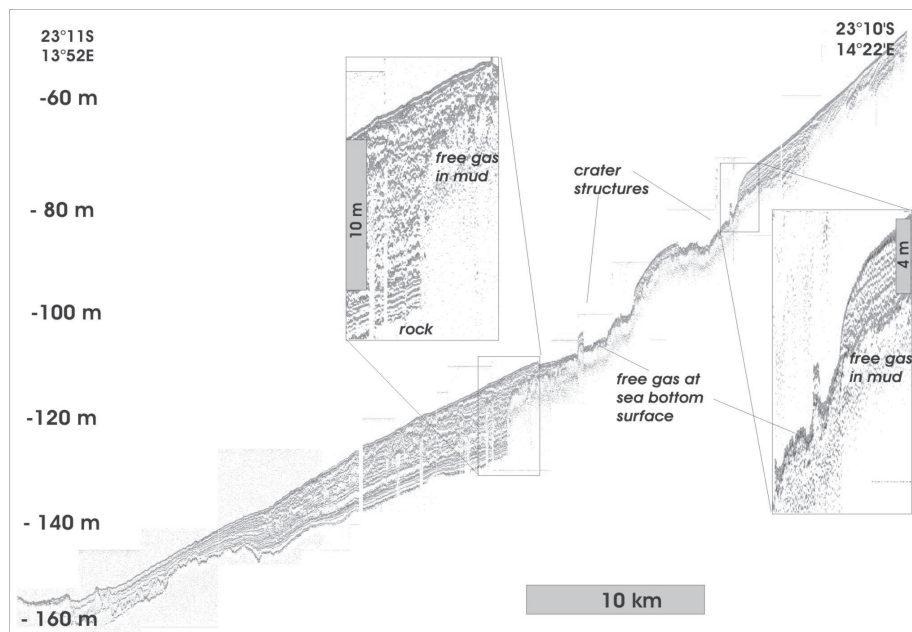


Figure 11. SES96 Sediment echosounder profile 2: cross section of the mud belt at 23° 10'S, showing pockmark/crater structures and abundant gas blankings.

pockmark structures covers about 380 km<sup>2</sup>. Pockmarks occupy 5 to 10 percent of this area. The total gas-filled area has been estimated to cover as much as 1350 km<sup>2</sup> [14]. Free gas in the shelf sediments is restricted to an area between 22°S and 23°15'S between 40 m and 120 m water depth. Outside this area, a small patch was detected off Conception Bay at 24°S. Our data coverage is considered sufficiently tight to predict that no large gas-filled areas have remained undetected between 22° and 27°S.

## 7. TRANSPORT MECHANISMS OF HYDROGEN SULPHIDE TO THE WATER COLUMN

### 7.1 Catastrophic Methane Eruptions

Video observations of rising gas bubbles, sediment craters, and disrupted seafloor off Walvis Bay suggest locally enhanced transport of hydrogen sulphide and methane by eruptive degassing. A budget assessment of the available amount of hydrogen sulphide in the sediments is instructive to estimate the reservoir strength of the mud belt for the supply of hydrogen sulphide to the overlying water column. The gas-charged sediments, which cover 1350 km<sup>2</sup> (Table 2a) would contain about  $2.0 \cdot 10^{11}$  moles hydrogen sulphide, if porewater

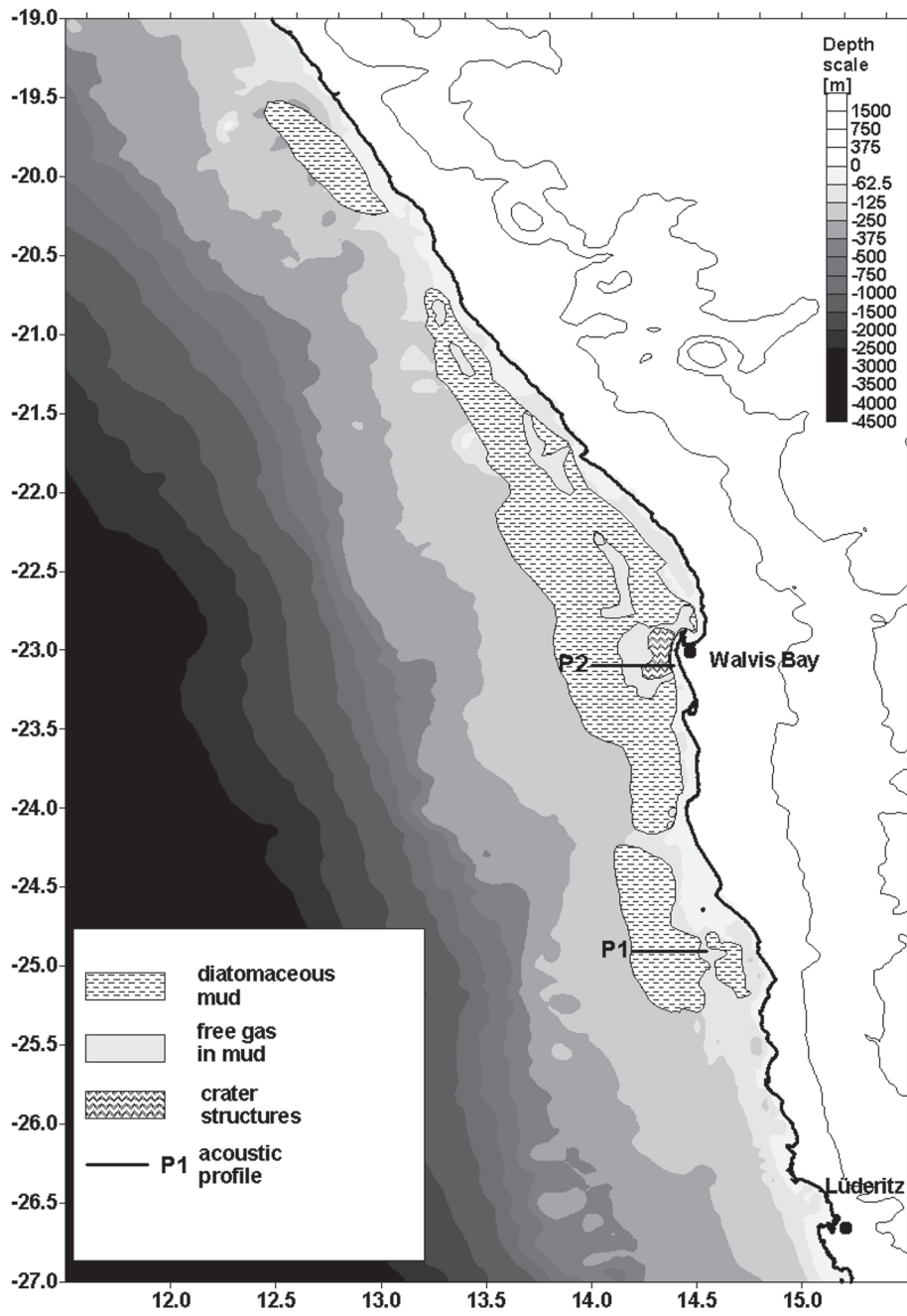


Figure 12. Distribution map of diatomaceous mud and gas-charged area. The area with abundant crater structures and disrupted seafloor is highlighted in dark-grey.

sulphide concentrations in the methane-containing zone are 15 mM [14]. Areal integration of the amount of hydrogen sulphide in the water column yielded an estimated  $0.3$  to  $0.8 \times 10^9$  moles of hydrogen sulphide. Only between 0.2 and 0.4 % of this reservoir is required to replenish the bottom water with hydrogen sulphide to concentrations exceeding  $1 \mu\text{M}$ .

We assessed the amount of hydrogen sulphide that would have been released during a violent sediment eruption, using as an example a crater with a diameter of 250 m and a depth of 10 m, which was mapped during METEOR expedition M57-3 [42]. The total volume of sediment missing from this crater is about  $490,000 \text{ m}^3$ . If this volume of sediment had an average porewater hydrogen sulphide concentration of 15 mM and a porosity of 0.8, then the total amount of hydrogen sulphide in the crater void would have been  $5.9 \times 10^6$  moles. Assuming that the overlying seawater contained at least  $6 \mu\text{moles}$  of hydrogen sulphide per litre seawater, about  $10^{12}$  litres of seawater could contain this concentration of hydrogen sulphide. For a water depth of 60 meters, this corresponds to an area covering 16 square kilometres. The calculation indicates that individual sediment eruptions may have an important local impact on hydrogen sulphide in the water column, but are of limited regional significance.

Sediments, which contain no free gas or free gas at more than 3 m sediment depth at the time of the acoustic echosounding surveys, have not likely emitted gas to the overlying water column in the past years. The size and outline of the gas-charged areas identified on echosounding lines conducted on cruises in August 2000, March 2003, and March 2004 coincide closely. Gas-free areas and areas with free gas at more than 3 m sediment depth all have good sediment stratification [5], a lack of surface structures, and from the core samples examined, a deep penetration of dissolved sulphate (Fig. 13a). The profile shape of pore water sulphate in Fig. 13a suggests that the dominant mode of sulphate transport has been by molecular diffusion. If these sediments once contained free gas near the sediment surface, sulphate would have been depleted a few centimetres below the sediment surface. After the gas release, sulphate would have diffused downward. It would take approximately 180 years for sulphate to diffuse over a distance of 3 m by molecular diffusion [18]. In addition, in sediments with diffusive interfaces between methane and sulphate more than 95 percent of the methane is oxidized anaerobically with sulphate, which counteracts the build-up of gas overpressure. For these reasons, it is unlikely that undisturbed areas surveyed have in the past contributed to methane gas emission.

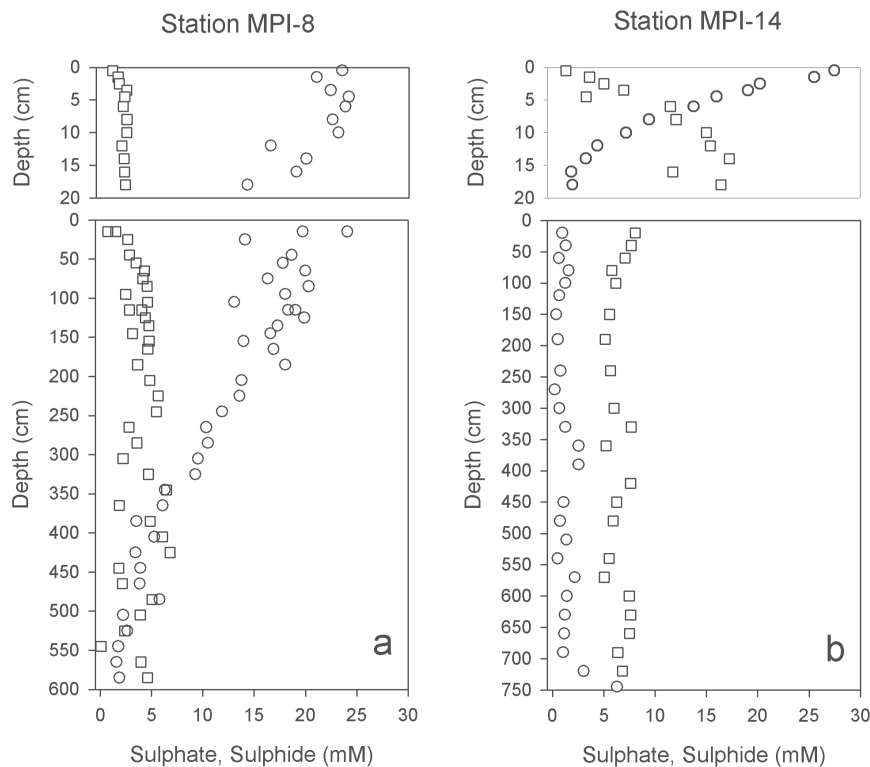


Figure 13. Comparative depth profile of sulphate and sulphide concentrations (a) from an area devoid of free gas (left profile) and (b) from an area where the gas-charged zone almost intercepts with the sea floor. ● (sulphate, multi-core), ○ (sulphate, gravity core), ■ (sulphide, multi-core), □ (sulphide, gravity core).

## 7.2 Methane Ebullition

Apart from catastrophic eruptions, advective transport due to methane ebullition in gas-charged areas would also enhance the exchange between sediment and seawater. Several studies have demonstrated that gas advection enhances pore water transport [22, 23, 28]. Co-transport of porewater methane and hydrogen sulphide is evident from the concentration profiles in one of the craters (Fig. 6 and 13b). The porewater profiles are linear just below the sediment surface and show highly significant correlations between hydrogen sulphide and methane. These profile shapes suggest mixing and advective transport of porewater and gas. The pH values of the porewaters range between 7.0 and 7.4. In this pH range, between 25 and 45 percent of dissolved sulphide is present as hydrogen sulphide gas, which can be transported together with methane. The

actual fluxes of hydrogen sulphide across the sediment-water interface in the gas-charged sediments are therefore likely higher than those calculated from molecular diffusion. However, gas bubbling on the Namibian shelf is apparently intermittent. An areal and temporal quantification of the fluxes during active gas emission has not yet been studied and remains difficult, because neither the rate of advection nor the frequency of such gas emissions is known.

### **7.3 Bottom Water Hydrogen Sulphide Replenishment by Production of Hydrogen Sulphide in the Topmost Sediment Layers**

The area of gas-charged sediments is significantly smaller than the spatial occurrence of bottom water sulphide, and is much smaller than the area outlined by positive fluxes of hydrogen sulphide across the sediment-water interface (Table 2 and Fig. 7b). Gas-charged sediments occur over a much smaller area than hydrogen sulphide-containing waters. In particular, bottom water sulphide has often been observed as far south as 26°30'S [40], where gas saturation occurs in more than 6 m sediment depth (Fig. 13a). These observations suggest that processes other than ebullition and gas eruption are of significance for the production of water column hydrogen sulphide.

In shelf areas with less than 100 m water depth, sulphate reduction rates in the topmost 20 cm are high enough to generate a hydrogen sulphide flux that can produce  $\mu\text{M}$  concentrations of hydrogen sulphide in the bottom waters within a few days. In this process hydrogen sulphide is essentially inexhaustible because continuous replenishment of fresh deposited organic matter and short diffusion distance for seawater sulphate maintain the microbial production of hydrogen sulphide at the sediment surface. Using the areal estimates of 27978  $\text{km}^2$  for bottom hydrogen sulphide and the hydrogen sulphide fluxes calculated for this area (Table 2), it would take a maximum of 7.5 days to reach a sulphide concentration of 1  $\mu\text{M}$  in a 10 m thick bottom water layer for the whole area. However, since the flux estimate is taking the whole area into account, in areas with significantly higher fluxes, locally bottom water hydrogen sulphide would accumulate much faster.

Key requirements for this process are a bottom boundary layer water that is stagnant and that contains very little dissolved nitrate and oxygen. Under these circumstances, bacterial sulphide oxidation with oxygen and nitrate is inhibited and the diffusive flux of sulphide from the sediment into the bottom waters is enhanced. Episodic in-shore movement and upward mixing of the bottom boundary layer would transport hydrogen sulphide into the oxic part of the water column where turbulent mixing with oxygen produces the colloidal elemental sulphur.

## 8. Summary

Temporally and spatially variable circulation patterns control the development and persistence of an isolated, stagnant bottom boundary layer that contains low concentrations of oxygen and nitrate. Preconditions are low wind stress and distance from the Angola-Benguela Front in order to deplete nutrient-rich SACW of nitrate.

Aerobic respiration in the water column consumes the major amount of oxygen supplied by upwelling and primary production. Sediments account for 9 to 25 % of the oxygen consumption. The major source of hydrogen sulphide is the diatomaceous mud belt, where excess organic matter deposition supports bacterial hydrogen sulphide and methane production. Water column bacterial sulphate reduction was found to contribute little to the development of water column hydrogen sulphide.

For the development of bottom water sulphidic conditions, bacterial sulphide oxidation at the sediment-water interface must be inhibited or ineffective. These conditions are only met after complete depletion of nitrate in the bottom waters. The large sulphur bacteria *Beggiatoa* spp. would represent an effective barrier against hydrogen sulphide. Nitrate-consuming processes in the water column such as anammox contribute to the development of complete nitrate depletion.

The development of bottom water sulphidic conditions is accelerated by advective transport mediated by gas ebullition and during catastrophic eruption events. The structure of the Namibian shelf and slope sediments indicate that this mechanism is active in an area between 23°S and 24°S in water depths less than 100 m.

The temporal and spatial variability of water column hydrogen sulphide occurrences suggest that several mechanisms are active on the shelf. The in-shore area may be affected more strongly by gas ebullition, whereas the central shelf probably experiences mainly diffusive supply of hydrogen sulphide to the bottom waters. Possible linkages between the gas emanations and wind-driven circulation remain the subject of further research.

## Acknowledgements

We would like to thank Lev Neretin for the invitation to contribute to this book and the two reviewers for their constructive comments. Tim Ferdelman provided unpublished data on sulphate reduction rates from 1997, and Daniela Riechmann provided bacterial counts from the METEOR cruise M48-2. We are grateful for scientific discussions with Anja van der Plas, Bo Barker Jørgensen, Tim Ferdelman, Kay-Christian Emeis, Helle Ploug, Marcel Kuypers, Gaute Lavik, and Heide Schulz. Gerd Bening, Chibola Chiklililwa, Kirsten Imhoff, Swantje Lilienthal, Martina Meyer, Gerald Nickel, Andrea Schipper, the late Bernd Schulz, Heidi Skrypzeck, Monika Trümper, and Tamara Zemskaya pro-

vided technical assistance for this study. Funding was provided by the Max-Planck Society, the DFG Research Center Ocean Margins at the University of Bremen, the BMBF and DFG programme GEOTECHNOLOGIEN, the DFG priority programme 516 (Meteor expeditions), the Benguela Environment Fisheries Interaction and Training Programme BENEFIT, and the Ministry of Fisheries, Namibia. This is publication no. GEOTECH-175 of the GEOTECHNOLOGIEN programme of BMBF and DFG, Grant 03G0580B NAMIBGAS.

## References

- [1] Aller R.C. and Rude P.D. Complete oxidation of solid phase sulfides by manganese and bacteria in anoxic marine sediments. *Geochim Cosmochim Acta* 1988; 52:751-65.
- [2] Bailey G.W., Boyd A.J., Duncombe Rae C.R., Mitchell-Innes B. and van der Plas A. Synthesis of marine science research in the Benguela Current system during cruises linked to the BENEFIT training programme in 1999. *S Afr J Sci* 2001; 97:271-74.
- [3] Berg P., Petersen-Risgaard N. and Rysgaard S. Interpretation and measured concentration profiles in sediment pore water. *Limnol Oceanogr* 1998; 43:1500-10.
- [4] Bleil U. *Report and Preliminary Results of METEOR Cruise 34/1, Cape Town - Walvis Bay, 31.01.1996 -25.01.1996*. Bremen, Berichte Fachbereich Geowissenschaften, Universität Bremen, 1996.
- [5] Borchers S.L., Schnetger B., Böning P. and Brumsack H.-J. Geochemical signatures of the Namibian diatom belt: Perennial upwelling and intermittent anoxia. *Geochem Geophys Geosy* 2005; 6:1-20.
- [6] Boyd A.J. Intensive study of the currents, winds and hydrology at a coastal site off central South West Africa, June/July 1978. Investigational Report, Sea Fisheries Institute, Republic of South Africa, 1983; 1-47.
- [7] Brüchert V., Jørgensen B.B., Neumann K., Riechmann D., Schlösser M. and Schulz H. Regulation of bacterial sulfate reduction and hydrogen sulfide fluxes in the central Namibian coastal upwelling zone. *Geochim Cosmochim Acta* 2003; 67:4505-18.
- [8] Brüchert V., Pérez M.E. and Lange C.B. Coupled primary production, benthic foraminiferal assemblage, and sulfur diagenesis in organic-rich sediments of the Benguela upwelling system. *Mar Geol* 2000; 163:27-40.
- [9] Campillo-Campbell C. and Gordo A. Physical and biological variability in the Namibian upwelling system: October 1997-October 2001. *Deep-Sea Res* 2004; 51:147-58.
- [10] Carr M.-E. Estimation of potential productivity in Eastern Boundary Currents using remote sensing. *Deep-Sea Res* 2002; 49:59-80.
- [11] Chapman P. and Shannon L.V. The Benguela Ecosystem Part II. Chemistry and related processes. *Oceanogr Mar Biol Ann Rev* 1985; 23:183-251.
- [12] Cline J.D. Spectrophotometric determination of hydrogen sulfide in natural waters. *Limnol Oceanogr* 1969; 14:454-59.
- [13] Emeis K.-C., Bening G., Berger J., Brüchert V., Currie B., Endler R., Ferdelman T., Finke N., Graco M., Haferburg G., Heyn T., Kiessling A., Lage S., Leipe T., Mollenhauer G., Neumann K., Nickel G., Noli K., Riechmann D., Schippers A., Schneider R., Schulz H., Shidjuu A., Sonnabend H., Stregel S., Struck U., Treppke U., Vogt T. and Zemskaya T. *Cruise Report Meteor Expedition M48-2, Walvis Bay - Walvis Bay, August 8 - August 23, 2000*. Bremen, Berichte Fachbereich Geowissenschaften Universität , 2002.



- [14] Emeis K.-C., Brüchert V., Currie B., Endler R., Ferdelman T.G., Kiessling A., Leipe T., Noli-Peard K., Struck U. and Vogt T. Shallow gas in shelf sediments of the Namibian coastal upwelling ecosystem. *Cont Shelf Res* 2004; 24:627-42.
- [15] Hamukuaya H., O'Toole M. and Woodhead P.M.J. Observations of severe hypoxia and offshore displacements of Cape Hake over the Namibian Shelf in 1994. *S Afr J Marine Sci* 1998; 19:41-57.
- [16] Hardman-Mountford N.J., Richardson A.J., Agenbag J.J., Hagen E., Nykjaer L., Shillington F.A. and Villacastin C. Ocean climate of the South East Atlantic observed from satellite data and wind models. *Prog Oceanogr* 2003; 59:181-221.
- [17] Helly J.J. and Levin L.A. Global distribution of naturally occurring marine hypoxia on continental margins. *Deep-Sea Res* 2004; 51:1159-68.
- [18] Jørgensen B.B. Bacteria and biogeochemistry, In *Marine Geochemistry*, H.D. Schulz and M. Zabel, eds. Berlin: Springer Verlag, 2000.
- [19] Kiørboe T. and Jackson G.A. Marine snow, organic solute plumes, and optimal chemosensory behaviour of bacteria. *Limnol Oceanogr* 2001; 46:1309-18.
- [20] Kiørboe T., Tiselius P., Mitchell-Innes B., Hansen J.L.S., Visser A.W. and Mari X. Intensive aggregate formation with low vertical flux during an upwelling-induced diatom bloom. *Limnol Oceanogr* 1998; 43:104-16.
- [21] Kuypers M.M.M., Lavik G., Woebken D., Schmid M., Fuchs B.M., Amann R., Jørgensen B.B. and Jetten M.S.M. Massive nitrogen loss from the Benguela upwelling system through anaerobic ammonium oxidation. *PNAS* 2005; 102:6478-83.
- [22] Martens C.S., Albert D.B. and Alperin M.J. Biogeochemical processes controlling methane in gassy coastal sediments-part 1. A model coupling organic matter flux to gas production, oxidation, and transport. *Cont Shelf Res* 1998; 18:1741-70.
- [23] Martens C.S. and Klump J.V. Biogeochemical cycling in an organic-rich coastal marine basin-I. Methane sediment-water exchange processes. *Geochim Cosmochim Acta* 1980; 44:471-90.
- [24] McHatton S.C., Barry J.P., Jannasch H.W. and Nelson D.C. High nitrate concentrations in vacuolate, autotrophic marine *Beggiatoa* spp. *Appl Environ Microb* 1996; 62:954-58.
- [25] Mohrholz V., Schmidt M. and Lutjeharms J.R.E. The hydrography and dynamics of the Angola-Benguela frontal zone and environment in 1999. *S Afr J Sci* 2001; 97:199-208.
- [26] Naqvi S.W.A., Jayakumar D.A., Narvekar P.V., Nalk H., Sarma V.V.S.S., D'Souza W., Joseph S. and George M.D. Increased marine production of N<sub>2</sub>O due to intensifying anoxia on the Indian continental shelf. *Nature* 2000; 408:346-49.
- [27] Nelson D.C., Jørgensen B.B. and Revsbech N.P. Growth pattern and yield of a chemoautotrophic *Beggiatoa* spp. in oxygen-sulfide microgradients. *Appl Environ Microb* 1986; 52:225-33.
- [28] O'Hara S.C.M., Dando P.R., Schuster U., Bennis A., Boyle J.D., Chui F.T.W., Hatherell T.V.J., Niven S.J. and Taylor L.J. Gas seep induced interstitial water circulation: observations and environmental applications. *Cont Shelf Res* 1995; 15:931-48.
- [29] Otte S., Kuenen J.G., Nielsen L.P., Paerl H.W., Zopfi J., Schulz H.N., Teske A., Strotmann B., Gallardo V.A. and Jørgensen B.B. Nitrogen, carbon, and sulfur metabolism in natural *Thioploca* samples. *Appl Environ Microb* 1999; 65:3148-57.
- [30] Ploug H., Hietanen S. and Kuparinen J. Diffusion and advection within and around sinking, porous diatom aggregates. *Limnol Oceanogr* 2002; 47:1129-36.



- [31] Poole R. and Tomczak M. Optimum multiparameter analysis of the water mass structure in the Atlantic Ocean thermocline. *Deep-Sea Res I* 1999; 46:1895-921.
- [32] Schippers A. and Jørgensen B.B. Biogeochemistry of pyrite and iron sulfide oxidation in marine sediments. *Gechim Cosmochim Acta* 2002; 66:85-92.
- [33] Schulz H.N., Brinkhoff T., Ferdelman T.G., Mariné H.M., Teske A. and Jørgensen B.B. Dense populations of a giant sulfur bacterium in Namibian sediments. *Science* 1999; 284:493-95.
- [34] Shannon L.V. and Nelson G. The Benguela: Large scale features and processes and system variability, In *The South Atlantic, present and past circulation*, Wefer G., Berger W., Siedler G. and Webb D. J., eds. Berlin: Springer, 1996.
- [35] Shillington F.A. The Benguela Upwelling System off south-western Africa, In *The Sea*, Robinson A.R. and Brink K.H., eds. New York: Wiley, 1998.
- [36] Spiess V. *Digitale Sedimentechographie-Neue Wege zu einer hochauflösenden Akustostratigraphie*. Bremen: Fachbereich Geowissenschaften, Universität Bremen, 1993.
- [37] Thamdrup B., Fossing H. and Jørgensen B.B. Manganese, iron, and sulfur cycling in a coastal marine sediment, Aarhus Bay, Denmark. *Geochim Cosmochim Acta* 1994; 58:5115-29.
- [38] Tyrrell T. and Lucas M.I. Geochemical evidence of denitrification in the Benguela upwelling system. *Cont Shelf Res* 2002; 22:2497-511.
- [39] Ulloa O., Escribano R., Hormazábal S., Quiñones R., Gonzales R. and Ramos M. Evolution and biological effects of the 1997-1998 El Niño in the upwelling ecosystem of northern Chile. *Geophys Res Lett* 2001; 28:1591-94.
- [40] Weeks S.J., Currie B., Bakun A. and Peard K.R. Hydrogen sulphide eruptions in the Atlantic Ocean off southern Africa: implications of a new view based on SeaWiFS satellite imagery. *Deep-Sea Res* 2004; 51:153-72.
- [41] Wilkens R.H. and Richardson M.D. The influence of gas bubbles on sediment acoustic properties: in situ, laboratory and theoretical results from Eckernförde Bay, Baltic Sea. *Cont Shelf Res* 1998; 18:1859-92.
- [42] Zabel M., Brüchert V. and Schneider R.R. *The Benguela Upwelling System 2003, Cruise No. 57, 20 January - 13 April 2003, Meteor Berichte*. Hamburg: Universität Hamburg, 2004.